JOURNAL OF CATALYSIS 74, 252–265 (1982)

Surface Characterization of the $Ru_3(CO)_{12}/Al_2O_3$ System

III. Surface Properties after Full Decarbonylation and Reduction

E. GUGLIELMINOTTI AND A. ZECCHINA

Istituto di Chimica Fisica, Università di Torino, Corso M. d'Azeglio 48, 10125 Torino, Italy

AND

A. BOSSI AND M. CAMIA

Istituto "G. Donegani" S.p.A., Via G. Fauser 4, 28100 Novara, Italy

Received May 22, 1981; revised November 11, 1981

The structure of dispersed Ru obtained by full decarbonylation of the $Ru_3(CO)_{12}/Al_2O_3$ system is discussed. Samples decarbonylated *in vacuo* are appreciably oxidized and trivalent anchored species are the main oxidized product. These Ru ions can act as nucleation centres for the formation of very small metallic particles which, due to their extremely reduced dimensions, can be broken up by CO at 473 K with formation of low-nuclearity anchored carbonylic complexes. By successive decarbonylation *in vacuo*, these complexes give back the initial metallic particles, so showing that highly dispersed Ru is mobile at 473 K. Samples decarbonylated in flowing H_2 do not show these features and this is explained by the larger dimensions of the metallic particles, which resist the CO attack.

INTRODUCTION

Al_2O_3-supported metallic ruthenium is normally prepared by impregnating the Al_2O_3 carrier with $RuCl_3$ and then reducing in flowing H_2 at $T \geq 623$ K. By using small metallic clusters such as $Ru_3(CO)_{12}$ as impregnant, it is hoped that more dispersed metallic phases can be prepared. In Part I (*1*), however, we have shown that by total decarbonylation *in vacuo* at 623 K of the $Ru_3(CO)_{12}/Al_2O_3$ system, a variety of anchored ruthenium species are present on the surface. On the most dilute samples (0.33%) ruthenium is mainly present in oxidized forms derived by oxidative attack of surface OH groups on surface carbonylic species. On more concentrated samples (1.57%) a more consistent fraction of zerovalent Ru is present, which derives from direct decarbonylation of $Ru_3(CO)_{12}$ not oxidized by surface OH groups. Decarbonylation in H_2 influences the relative ratios of the oxidation states of ruthenium favouring more reduced situations. Even if the ruthenium compound used for the impregnation process is originally in the zerovalent state, the resulting phase after total decarbonylation is (at least *in vacuo*) appreciably oxidized. In the present paper a spectroscopic study is carried out in order to investigate whether the reduction of such an oxidized phase can lead to more dispersed metallic phases.

EXPERIMENTAL

All the experimental details are as described in Parts I and II (*1*, *2*).

RESULTS

CO Adsorption and Desorption

In Fig. 1a the ir spectra of CO adsorbed on 0.33 and 1.57% samples decarbonylated *in vacuo* and on a 1.57% sample decarbonylated in flowing H_2 are compared (solid curves). It can be seen that: (i) in contrast with the 0.33% samples, the CO adsorbed on the 1.57% samples treated *in vacuo*

0021-9517/82/040252-14$02.00/0

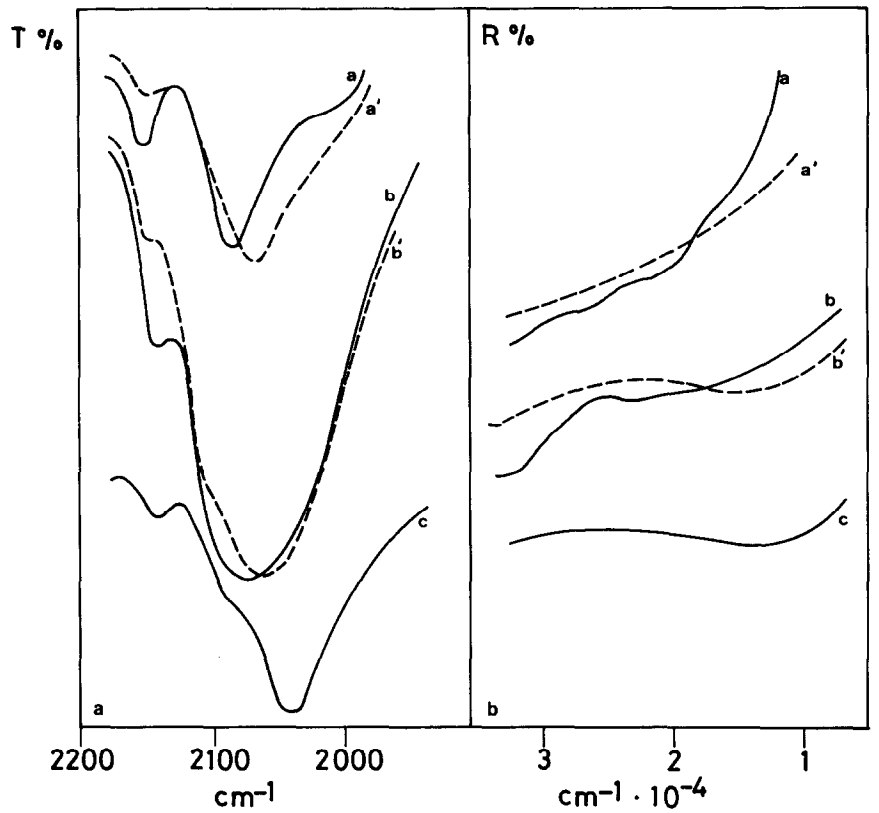

FIG. 1. (a) Comparison between the ir spectra of adsorbed CO on samples before reduction (a, b) and after reduction (a', b') (0.33%, 1.57%). Spectrum c corresponds to CO adsorbed on a 1.57% sample reduced in flowing H_2. (b) The uv–vis reflectance spectra before (a, b) and after (a', b') reduction (0.33% and 1.57%) and of a sample reduced in flowing H_2 (c).

gives rise to a broad absorption centred at ~2070 cm^{-1}; (ii) the integrated intensity of the CO adsorbed on 1.57% samples treated in flowing hydrogen is much smaller in comparison with that of the same sample treated *in vacuo*; (iii) on all samples the characteristic bands of Ru_A complexes are observed with relative intensity decreasing in the order 0.33% (*in vacuo*), 1.57% (*in vacuo*), and 1.57% (H_2).

The effect of H_2 reduction at 623 K on the adsorption capacity towards CO is illustrated by the dashed curves. With respect to the unreduced samples the main differences are: (i) the intensity of Ru_A pairs decreases; (ii) the frequency of the strongest band shifts from 2060 (0.33%) to 2052 (1.57% *in vacuo*) and to 2040 cm^{-1} (1.57% decarbonylated in flowing H_2); (iii) the overall integrated intensity of CO adsorbed on 1.57% samples is much stronger on those previously activated *in vacuo* than on those decarbonylated in flowing H_2.

In Fig. 1b the parallel reflectance spectra carried out on CO-free samples both before and after reduction are illustrated. It can be seen that the effect of reduction is to decrease the intensity of the bands at frequencies higher than 18,000 cm^{-1} (which mainly belong, as already discussed, to oxidized species) with formation of broad bands at lower frequencies. The band maxima of these new more reduced species tend to shift progressively to lower frequencies on passing from 0.33 to 1.57% samples (both previously activated *in vacuo* or decarbonylated in flowing H_2).

In Fig. 2a the ir spectra taken at increas-

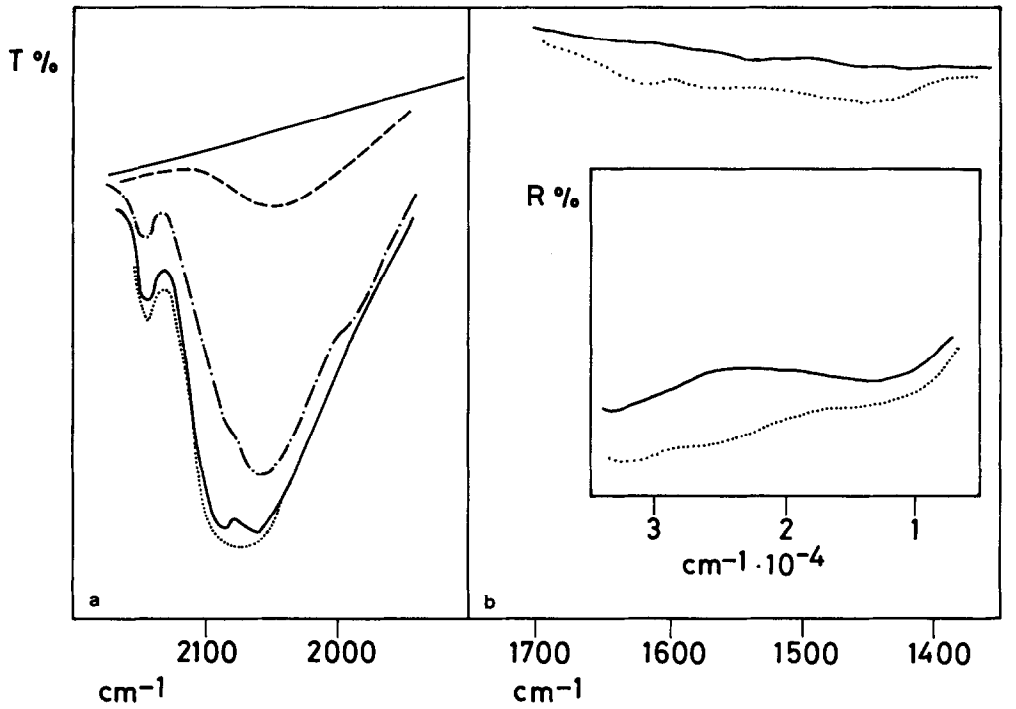

FIG. 2. Infrared spectra at increasing values of CO adsorbed on a 1.57% reduced sample: (a) range 2200–1900 cm^{-1}; (b) range 1700–1400 cm^{-1}. Inset: reflectance spectrum before and after CO (5.3 kPa) adsorption (full coverage).

ing CO coverages are illustrated for a 1.57% sample activated and reduced in the standard way. At very low coverage (dashed curve) the Ru_A pair is missing and only a broad maximum is observed at 2050 cm^{-1}. At larger coverages the Ru_A pair becomes clearly visible superimposed on the broad band whose maximum progressively shifts to 2060 and 2064 cm^{-1}, respectively (dot-dashed and solid curves). Finally at full coverage (dotted curve) the second component of the Ru_A pairs is no longer visible being obscured by the adjacent and more intense broad component: the resulting maximum is thus located at 2070 cm^{-1}. It should be noted that in all spectra a shoulder at 2000–1980 cm^{-1} cm is always visible. In Fig. 2b the effect of CO adsorption at full coverage in the range 1700–1300 cm^{-1} is illustrated. A broad and weak absorption with relative maxima at 1630, 1570, and 1450 cm^{-1} is observed, which is probably due to carbonate-like species. In the Fig. 2b inset, the effect of CO adsorption (full coverage) on the uv–vis–nir spectrum is shown: the overall intensity increases in the whole range 10,000–35,000 cm, but particularly so at ~25,000 cm^{-1} (as already observed in Part I).

Figure 3 shows the effect of CO desorption at increasing temperature on the ir spectrum of adsorbed CO. The results are quite surprising: completely new bands at 2030 and 2000 cm^{-1} (dashed curve) and at 2023 and 1986 cm^{-1} (dot-dashed curve) appear in desorption which were absent in the adsorption experiment illustrated in Fig. 2. These results indicate that, due to the effect of the temperature increase, new species are formed. In other words, this is not a true desorption experiment, but at least partially an activated process leading to new adsorbed structures.

In order to prove this hypothesis the following experiment has been carried out. A standard 1.57% reduced sample was previ-

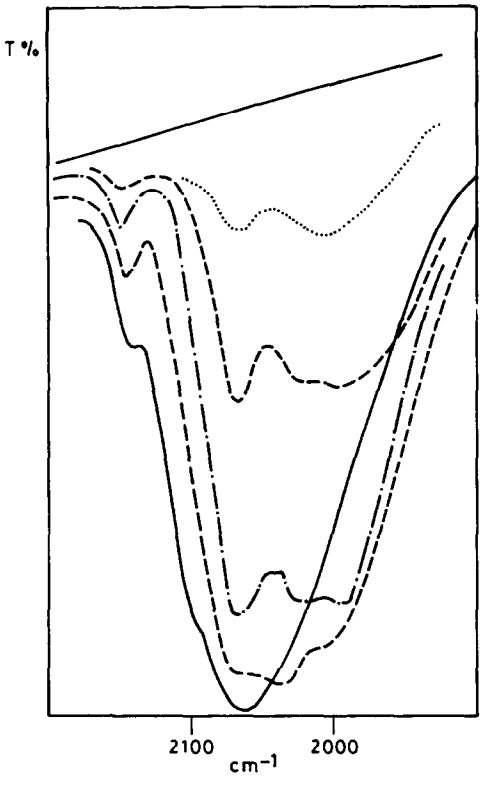

FIG. 3. Desorption experiment. Lower solid curve: initial ir spectrum; lower dashed curve: spectrum after desorption at 353 K; dot-dashed curve: spectrum after desorption at 423 K. The other curves refer to desorption at 473 K for increasing times.

ously fully covered with CO at RT; then, without removing the CO gas phase, the temperature was increased to 473 K. The result (Fig. 4a) was a new band at 2005 cm^{-1} together with a shoulder at 1970–1980 cm^{-1}. Although these bands are not identical to those found in Fig. 3 (which were obtained under different CO pressure) this experiment clearly demonstrated that the temperature increase favours the formation of new species.

In Fig. 4b the effect of successive outgassing at 473 K is shown: the resulting spectrum is nearly identical to that already discussed in the experiment described in Fig. 11 of Part II and interpreted in terms of superposition of Ru_A, Ru_B, and Ru_C carbonylic species. It is also very relevant that successive exposure to CO at 473 K restores the initial situation and this effect is nearly indistinguishable from that already described in Part II (Fig. 11) concerning the experiment of addition of CO to Ru_C complexes. Moreover, parallel volumetric measurements confirm these purely spectroscopic observations as the amount of adsorbed CO at 473 K on a 1.57% reduced sample is ~3–3.5 CO per Ru atom, i.e., the same value as determined in the experiment discussed in Part II. It is most noticeable that *all these phenomena are absent on samples decarbonylated in flowing* H_2.

CO Chemisorption in the Presence of H_2

So far the spectra concern the adsorption of CO at RT on samples reduced in H_2 at 623 K and then evacuated at the same temperature. In the experiment described in Fig. 5, a 1.57% sample (which underwent the reduction stage at 623 K) was cooled at RT in the presence of hydrogen (one atm) and the CO was bled in without removing the hydrogen atmosphere (dashed line). The highest component of the Ru_A complexes is strongly weakened in comparison to the typical result of a standard treatment (solid curve), i.e., H_2 has a strong inhibiting effect on CO chemisorption on Ru_A sites. Moreover, as the CO spectrum is slightly shifted to lower frequencies it is inferred that H_2 chemisorption also influences the adsorption of CO on the metallic sites.

Effect of O_2 *on Chemisorbed CO*

This experiment is described in Fig. 6 and has been carried out as follows. A standard 1.57% reduced sample fully covered with CO at RT (solid curve) is exposed to O_2 (5.3 kPa) at RT and the ir spectrum taken immediately and after 20 min (dotted and dot-dashed curves). It can be observed that: (i) the low-frequency part of the spectrum (~2060 cm^{-1}) is eroded; (ii) the peaks at 2134 and 2070 cm^{-1} due to Ru_A complexes increase; (iii) the peak at 2005 cm^{-1} also reveals the presence of Ru_B com-

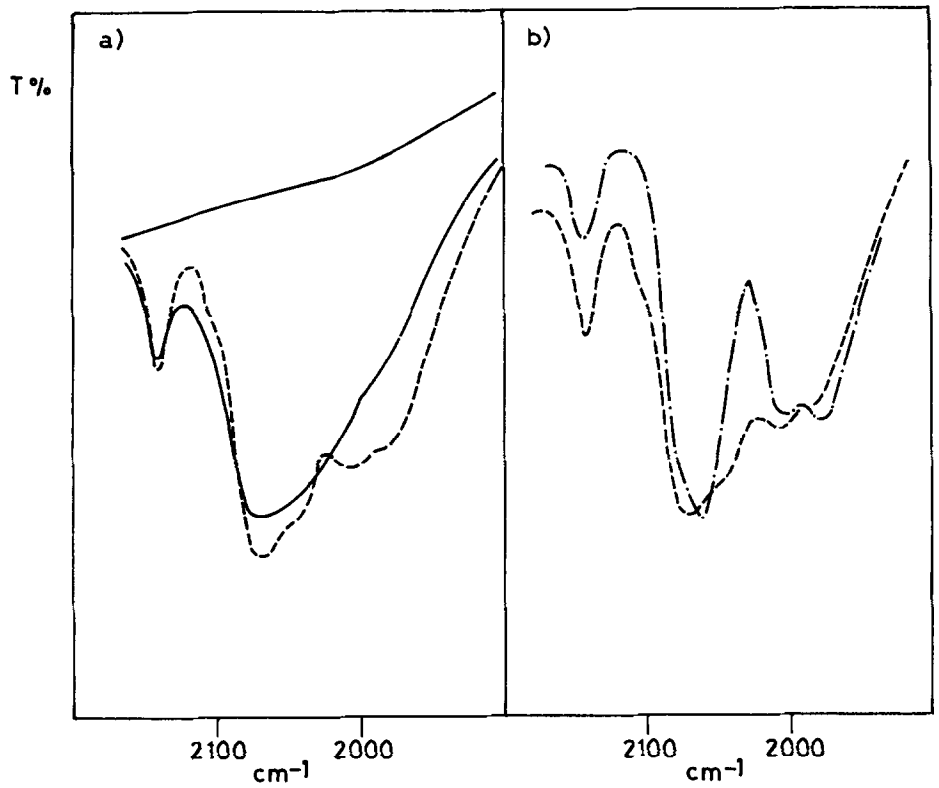

FIG. 4. (a) Upper solid curve: background of a 1.57% sample reduced in H_2; lower solid curve: spectrum of adsorbed CO at full coverage; dashed curve: after heating in CO (5.3 kPa) at 473 K. (b) Dashed curve: after heating in CO at 473 K; dot-dashed curve: after desorption for 10 min at 473 K.

plexes. Finally, after oxygen contact at RT the spectrum can be interpreted as mainly due to Ru_A and Ru_B oxidized dicarbonylic species. Further temperature increases lead to the gradual disappearance of both species in agreement with the results already discussed in Part II.

Oxidizing Effect of Surface OH Groups at High Temperature (773 K)

A 1.57% sample reduced in a standard way (and showing the typical CO spectrum illustrated in Fig. 7) (solid curve), is outgassed at 773 K and then contacted again with CO at RT in order to monitor the oxidizing state of the surface. The resulting spectrum (dashed curve) shows only the bands typical of Ru_A complexes, slightly displaced from their normal positions; moreover, the strong low-frequency broad band has disappeared. As this absorption is only found on samples containing reduced ruthenium, it is inferred that the treatment at high temperature is equivalent to an oxidation process. Due to the total exclusion of oxygen in all stages of the experiment, we are forced to conclude that the oxidizing agents are the surface OH groups. The resulting phase is very difficult to reduce in H_2. In fact after reduction in H_2 in the interval 623–773 K, exposure to CO does not give rise to the normal spectrum of CO on reduced samples, thereby suggesting that the oxidized phase is very stable.

Average Oxidation State after Reduction in H_2 at 623 K

A typical temperature-programmed reduction (TPR) experiment is shown in Fig. 8 for a 0.33% sample activated in flowing

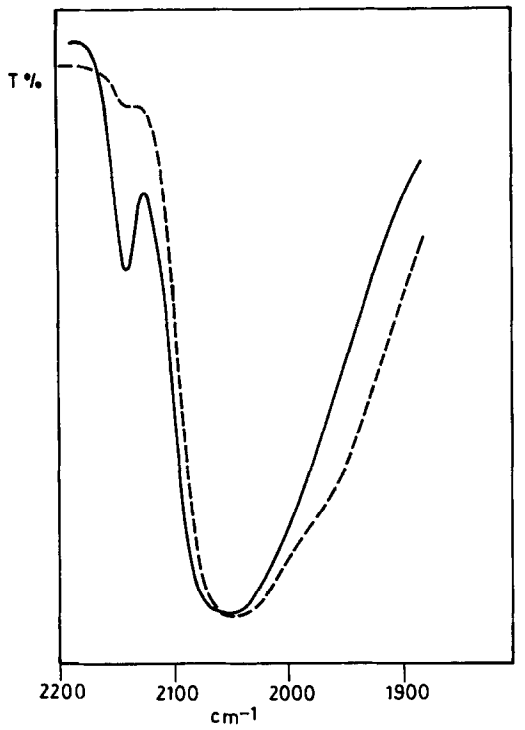

FIG. 5. Spectrum of CO adsorbed on H_2-covered surface (dashed curve) compared with that of CO adsorbed on reduced and outgassed surface (solid curve) (1.57% sample).

helium at 623 K. It can be seen that two reduction peaks are observed at 373 and 693 K. The temperature of the first reduction peak is very near to that of supported RuO_2 on the basis of data for the RuO_2 phase (see Fig. 5 of Part II). From its area it is inferred that approximately 25% of Ru is in the tetravalent state, while the remaining 75% is likely to be in the trivalent state which is very stable and can be reduced only at $T \geq 600$ K.

These considerations give information on the oxidation state before reduction in H_2 at 623 K. On the basis of the experiment reported in Fig. 8, after reduction in H_2 at 623 K the situation is modified such that ~30% of the total is in the zerovalent state while ~70% is in the trivalent state. These figures must be considered as only qualitative because intermediate oxidation states are not taken into consideration. The ratio between Ru^0 and Ru^{III} after reduction at 623 K is likely to be influenced by the ruthenium concentration. In particular we think that on more concentrated samples zerovalent ruthenium is definitely more abundant.

NO Adsorption

In Fig. 9 are reported the spectra of NO adsorbed on 1.57% samples, respectively, reduced in H_2 at 623 K (a), activated *in vacuo* at 623 K (b), and oxidized at 373 K (c). The results can be summarized as follows.

(*a*) *Reduced samples.* The spectrum of adsorbed NO is very complex and coverage dependent. In particular components are observed at 1860–1840, 1810–1800, 1690, and 1600 cm^{-1}. Among them the component at 1810–1800 cm^{-1} is present only at low coverages (it is destroyed when the NO coverage reaches the highest values) and

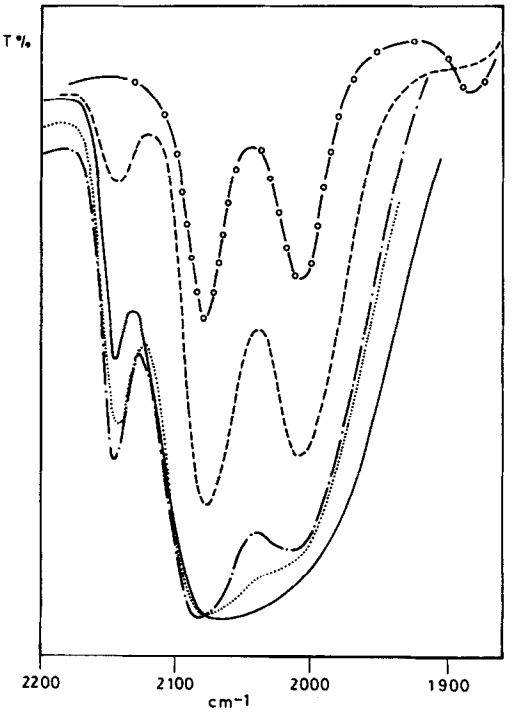

FIG. 6. Interaction of adsorbed CO (solid curve) (1.57% sample) with oxygen (5.3 kPa) at RT (dotted and dot-dashed curves) and at 353 (---) and 423 K (-o-).

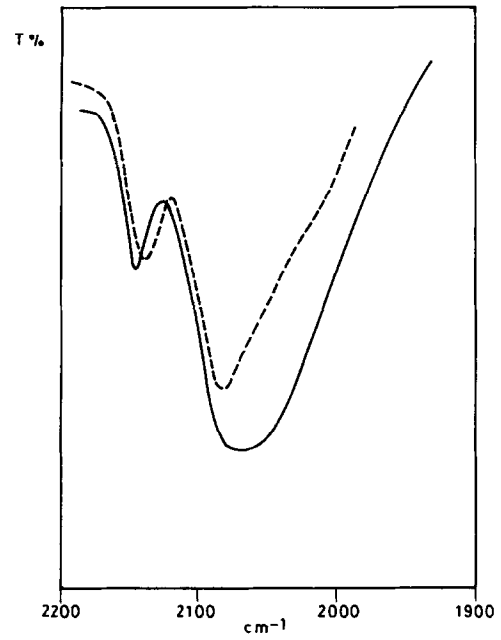

FIG. 7. Oxidizing effect of OH groups at 773 K. Solid curve: spectra of CO adsorbed on a 1.57% sample reduced at 623 K in H_2. Dashed curve: spectrum of CO adsorbed on a sample treated as before and then outgassed at 773 K.

the band at 1690 cm^{-1} is pressure dependent.

(*b*) *Activated samples.* The spectrum is very similar to the previous one. The only difference is that the frequencies of some components are definitely higher (1873, 1700 cm^{-1}).

(*c*) *Oxidized samples.* The spectrum is simpler with only one intense band at 1890 cm^{-1} and a weak component at ~1600 cm^{-1}. A comparison of the three spectra suggests an empirical correlation between the bands falling in the range 1820–1600 cm^{-1} and the concentration of ruthenium in low or zerovalent state.

Interaction of NO with Adsorbed CO

This interaction is illustrated in Fig. 10 for a 1.57% sample reduced in a standard way. The first NO dose erodes the low-frequency part of the CO spectrum and produces nitrosylic bands at 1840, 1810–1800, and 1730 cm^{-1}. At the same time the intensity of the Ru_A species increases. The effect of further doses can be summarized as follows: (i) the peaks initially formed are destroyed (this fact is particularly evident for the 1810 to 1800 cm^{-1} bands); (ii) new peaks at 1873 and 1700 cm^{-1} become prominent; (iii) after the initial increase the Ru_A species gradually decrease.

DISCUSSION

Spectrum of CO Adsorbed on Reduced Phases: Comparison with That Obtained on the Activated Ones

The obvious effect of reduction is to increase the relative amount of ruthenium in low oxidation state: as a consequence the concentration decrease of Ru_A complexes (where the ruthenium is thought to be trivalent) is not unexpected. Moreover, the parallel increase of the large absorption at 2070–2000 cm^{-1} monitors the formation of more reduced species. Comparison with the results for CO adsorbed on metallic Ru particles (*3–5*) strongly suggests that the broad absorption at 2070–2000 cm^{-1} can be assigned to CO linearly bonded to dispersed Ru in the zerovalent state. The gradual frequency change to lower frequencies of the apparent maxima on passing from 0.33 to 1.57% samples (reduced in the standard way and in flowing hydrogen, respectively) can be explained in several ways. Thus (i)

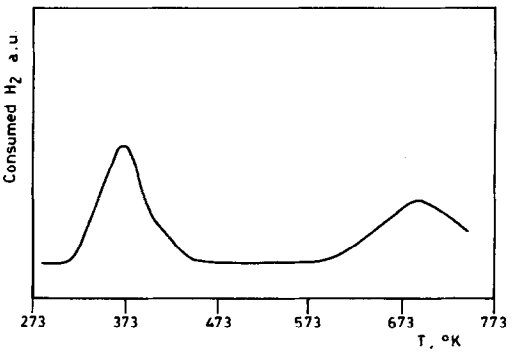

FIG. 8. Temperature-programmed reduction (TPR) of a 0.33% sample activated *in vacuo* at 623 K.

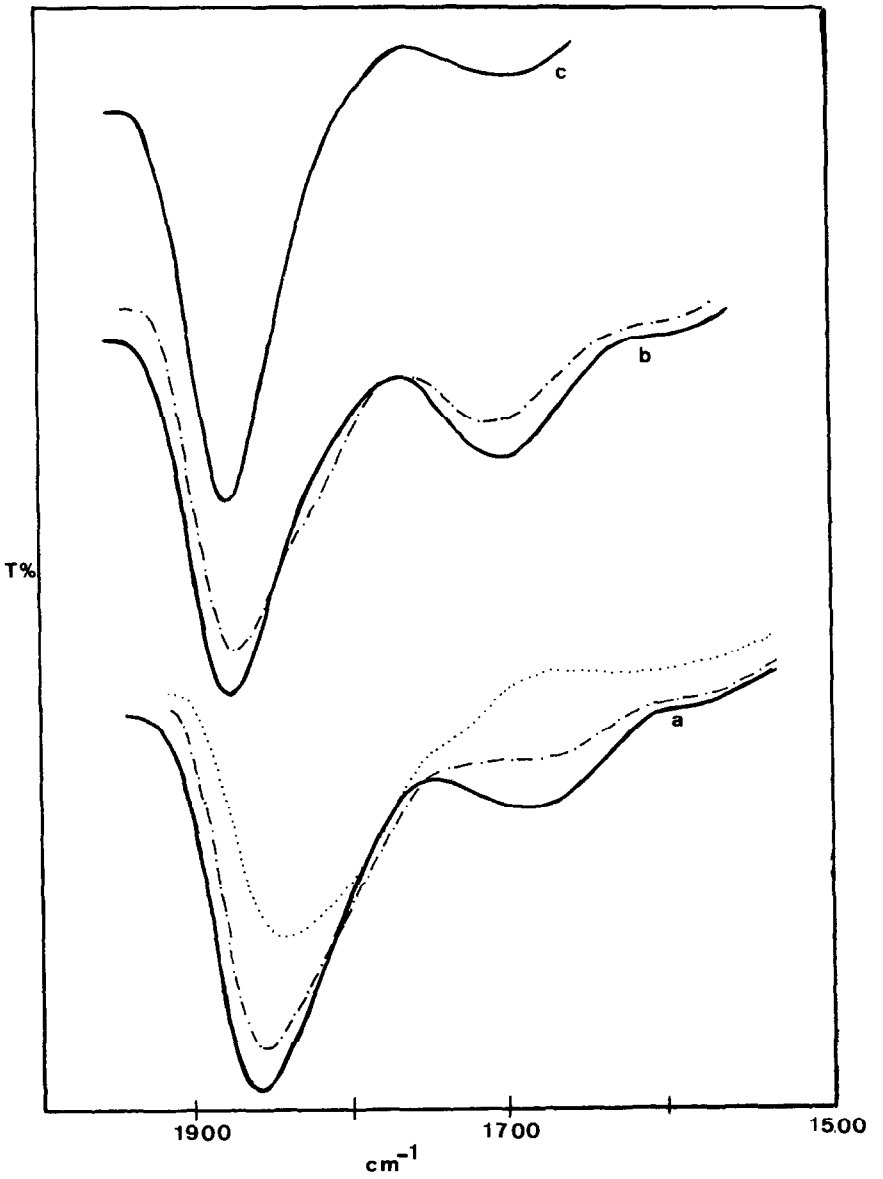

FIG. 9. NO adsorption on samples activated in different ways: (a) dotted curve: 1.3 kPa NO on a 623 K H_2-reduced (1.57%) sample; – · – and solid curve: 1.3 kPa NO immediately after contact and 1 hr later. (b) dot-dashed curve: 1.3 kPa NO on a 623 K activated *in vacuo* (1.57%) sample immediately after contact; solid curve: after 1 hr. (c) 1.3 kPa NO on a 373 K oxidized (1.57%) sample previously activated in a standard way.

the decrement is associated with an increase in the particle dimensions which causes a gradual increase of electron density on Ru atoms (*6*); (ii) the decrement is due to electron density changes caused by gradual variations in the oxidation state of the adsorbing centers; (iii) the decrement is due to both effects. The sample treated in flowing H_2 shows the smallest intensity and the lowest frequency of adsorbed CO and these findings can indeed be explained by the larger dimensions of the particles (as

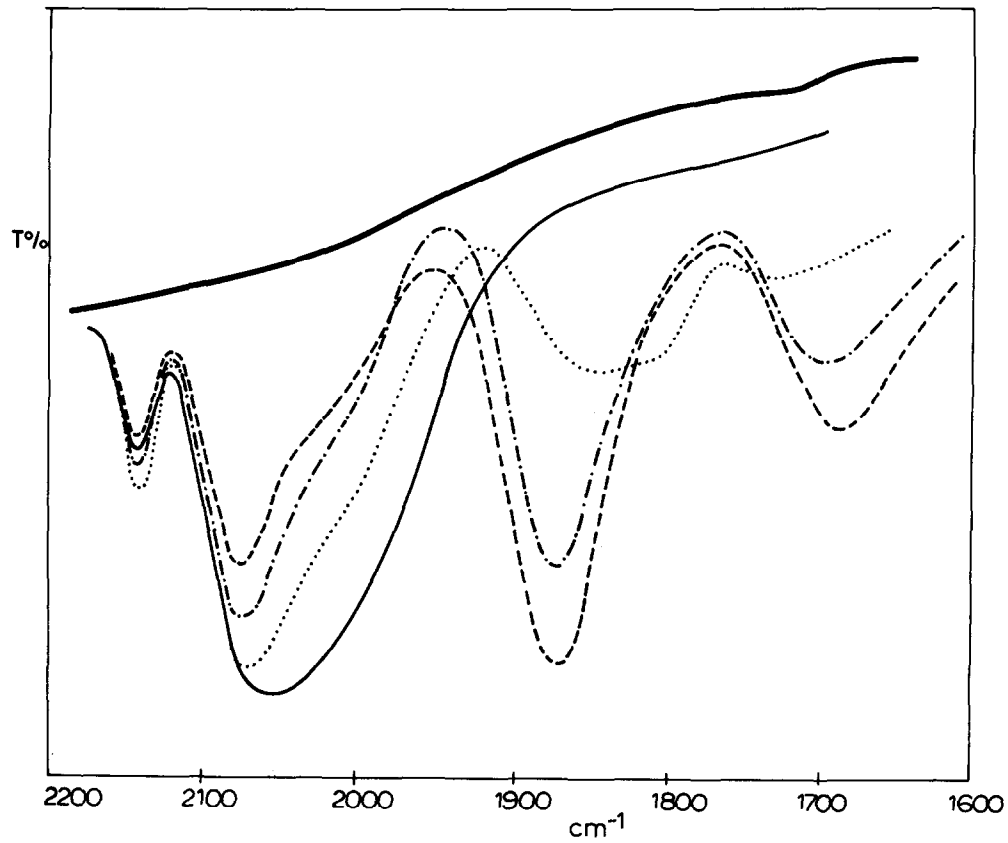

FIG. 10. Interaction of NO with preadsorbed CO. Upper solid curve: background after 623 K activation and H_2 reduction of a 1.57% sample; lower solid curve: saturated with CO; dotted, dot-dashed and dashed curves: spectra taken after contacting with 0.13 and 1.3 kPa NO (immediately and 1 hr later).

proposed in (i)). However, the correct hypothesis must not only account for the observed frequency shift but must also explain why the same sample (1.57%) has larger dispersion (and consequent higher intensity of adsorbed CO bands) when it is previously activated *in vacuo* as opposed to being decarbonylated in flowing hydrogen. A probable explanation is that during the activation *in vacuo* high oxidation states of Ru are generated by interaction with OH groups. The ions so formed are strongly anchored on the alumina surface because of their stabilization in a surface spinel-like or aluminate structure. As a consequence the successive treatment in H_2 transforms only a fraction of them into metallic ruthenium (see TPR experiment, Fig. 8). Following Yermakov's view (*7*), these samples should therefore contain a large number of nucleation centres (Ru^{x+} ions) which can bond Ru^0 atoms through Me–Me bonds, keeping the dispersion very high (as observed in other cases) (*8–10*). The metallic clusters generated in this way contain both Ru^{x+} and Ru^0 atoms in the same aggregate and this fact makes the situation of the average oxidation state of Ru in the cluster very uncertain. On this (qualitative) ground it can be safely stated that (i) the higher the concentration of nucleation centres the higher the dispersion and (ii) the smallest particles nucleated around positively charged Ru ions should carry a positive charge and hence have smaller electron density on exposed Ru atoms. As a conse-

quence the shift to higher frequency of the CO stretching mode (which is a sensitive probe of the electron density on adsorbing centres) is due to the contemporary action of the decrease in particle dimension and increase of the positive character of the particle (grown around the positive nucleation centres).

In flowing H_2 the formation of Ru^{x+} ions by reaction with surface OH groups is strongly inhibited. As a consequence few nucleation centres are generated and the metallic ruthenium can easily coalesce into larger aggregates, whose surface electron density thereby reaches the largest values. The merit of this hypothesis is that it can explain both the increase in dispersion and the parallel increase of the CO stretching modes. On the basis of the previous hypothesis the following qualitative picture of the surface emerges:

(*a*) *0.33% samples activated in vacuo.* A variety of oxidation states (IV and III) is present. Hydrogen immediately reduces the ruthenium present as the RuO_2-like phase and (at higher T) also a fraction of Ru^{x+} ions: the resulting situation is characterized by ~30% of Ru in the metallic state nucleated in very small clusters on anchored Ru^{x+} ions (which represent ~70% of the total).

(*b*) *1.57% samples activated in vacuo.* The picture is the same, the only difference being a larger amount of metallic ruthenium coming from direct decarbonylation of $Ru_3(CO)_{12}$ without previous oxidation by OH groups. Indicative figures cannot be given. However, the clusters are still very small, as the CO coverge indicates.

(*c*) *1.57% samples activated in flowing H_2.* The average oxidation state is very near zero and a high percentage of Ru is in metallic particles of larger dimensions.

As far as the effects of reduction on the reflectance spectra are concerned the following comments can be made:

(a) the erosion of the bands at $\bar{\nu} \geq 18{,}000$ cm^{-1} is due to reduction of oxidized species (cf. Part I) or destruction of absorption associated with dimeric or trimeric metallic clusters (*11, 12*);

(b) the absorption increase at $\bar{\nu} \geq 18{,}000$ cm^{-1} (with apparent broad maxima at 13,000 and 12,000 cm^{-1} on 1.57% samples previously activated *in vacuo* or immediately reduced in flowing H_2) is associated with more reduced species. We think that these absorptions are due to metallic particles as observed for other systems (*13, 14*). In trimetallic and bimetallic Ru clusters, bands due to $\sigma \rightarrow \sigma^*$ transitions associated with Me–Me bonds are observed at 25,000–30,000 cm^{-1} (*11, 12*). As far as we are aware larger clusters have not been studied, but it is known that a red shift occurs with the increase of the cluster dimensions (*15, 16*). Moreover, large low-frequency absorptions of the Mie type (*17–20*) are also normally present in dispersed metallic systems and are known to move to lower wavelengths with the increase of the size, as observed in our case. Hence a plausible assignment is that the large absorptions formed upon reduction are associated with transitions in metal particles.

Coverage Dependence of the CO Spectrum

At full coverage the measured CO uptake at RT on samples previously activated *in vacuo* is ~0.8–1 CO per Ru atom, which indicates a nearly atomic dispersion (by atomically dispersed metal is intended an aggregation state where all the ruthenium atoms are on the surface as in very small metallic aggregates or rafts) (*21*). The broadness of the bands assigned to CO linearly bonded to surface Ru atoms in small metallic aggregates indicates *per se* that the surface is strongly heterogeneous. A variety of similar structures is therefore present on the surface. Metal atoms with large electron density are occupied first as is proved by the low value of the stretching modes of CO adsorbed at the lowest coverages. The bands due to CO adsorbed on Ru_A sites appear only after the second dose in agreement with their ascertained stability only in

the presence of a small CO pressure. The most intriguing result, however, is the appearance in the range 1700–1400 cm^{-1} of weak bands due to carbonate-like species. Two explanations can be offered: (i) carbonate-like species are formed because CO acts as a reducing agent for oxidized Ru ions anchored on the surface which have resisted the H_2 action at 623 K; (ii) a dismutation reaction occurs on Ru particles giving C species and adsorbed CO_2. As yet we cannot choose between the two possibilities. Finally, the reflectance spectrum deserves some comment, particularly the effect of CO adsorption in increasing the intensity of the whole spectrum. The main effect is observed at 25,000 cm^{-1} where the $\sigma \rightarrow \sigma^*$ transitions associated with Me–Me bonds in clusters of extremely small nuclearity are expected to absorb. Two possible explanations are: (i) the presence of ligands modifies the extinction coefficient of the optical transitions essentially localized on Me–Me bonds; (ii) extremely small clusters are formed during the CO adsorption by rupture of some of the Ru–Ru bonds in metal particles or rafts. The presence of the shoulder at 2000–1980 cm^{-1} (i.e., where polycarbonylic species absorb: see the following discussion) is in favour of the second hypothesis.

Effect of Temperature on the Spectrum of Adsorbed CO

The results shown in Figs. 3 and 4 show that by increasing the temperature new species are formed. In particular the Fig. 3 experiment shows that by heating in CO atmosphere, the typical manifestation of the CO linearly bonded to ruthenium atoms in small crystallites is eroded and characteristics of polycarbonylic species like Ru_C complexes are generated; moreover, these observations agree with the quantitative measurements (CO/Ru $\simeq$ 3–3.5). These facts can be explained as follows. At higher T, the process of disaggregation of crystallites (already starting at RT) with rupture of Me–Me bonds and formation of small nuclearity species is predominent. Polycarbonylic compounds are thereby generated which explains the very high CO/Ru ratio. Ru_A, Ru_B, Ru_C, and other (possibly mononuclear) polycarbonylic complexes are formed and their relative concentration probably reflects the original situation of the oxidation states of the surface ruthenium ions. This picture of the situation of Ru atoms in CO at 473 K implies a state characterized by high mobility where a dynamic equilibrium exists between Me–Me bond rupture and Me–CO formation which is dependent on temperature and CO pressure. This fact is not unexpected if the high enthalpy change associated with Me–CO bond formation (*15*) is taken into account. Thus *in vacuo* (i.e., in absence of CO ligands) Ru^0 atoms nucleate around Ru^{z+} nucleation centres. Adsorption of CO mainly gives rise to CO groups linearly bonded to exposed metal atoms, without extensive disruption of the metallic aggregates. At higher T, the aggregates are partitioned into smaller clusters and so some of the nucleation centres previously buried become exposed to CO, and Ru_B (and possibly Ru_A) surface complexes are then formed. In other words the metallic atoms initially clustered into aggregates spread on the surface giving rise to a bidimensional dispersion. It is most interesting that if CO is totally desorbed at 623 K the initial situation is totally restored, as is revealed by subsequent exposure to CO at RT, when the typical spectrum of CO on reduced ruthenium is produced. These phenomena occur only on samples previously treated *in vacuo* and thus show the maximum dispersion. On samples activated in flowing H_2 the particles have larger dimensions and more easily resist the CO attack.

CO Chemisorption in the Presence of H_2 Atmosphere

In the presence of H_2, the formation of Ru_A species (where Ru is in the oxidized state) is strongly inhibited. This fact can in principle be explained in terms of the re-

ducing effect of H_2 atmosphere which preserves the surface from contamination. In order to check if the presence of oxidized Ru species was due to insufficient cleanness of the standard vacuum systems, experiments have been carried out in an ultrahigh vacuum system where ultimate pressures of 10^{-6} Pa were reached; however, the spectra were completely unaffected. This fact is not surprising because we have seen that the OH groups of the alumina surface are the principal oxidizing agents and their presence is certainly not influenced by ultimate residual pressures ranging between 10^{-3} and 10^{-6} Pa. As a consequence the inhibiting effect of hydrogen must be explained in another way. In our opinion, the following equilibrium exists:

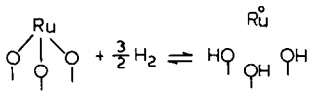

(1)

and this is shifted to the right in the presence of a hydrogen pressure. There is no direct experimental proof of the existence of this reaction because on a very hydroxylated surface the hypothetical formation of a small amount of new OH species would certainly escape ir observation. However, reaction (1) in the back direction describes the mechanism of attack on surface ruthenium atoms by OH groups to form oxidized aluminate phases. Moreover, on the basis of reaction (1) the effect of H_2 atmosphere in inhibiting the oxidative processes during the decarbonylation stage can be easily understood. Equilibria of this type have also been proposed for other systems (*22*).

Effect of Oxygen on the Spectrum of Adsorbed CO

By RT interaction of O_2 with adsorbed CO the broad bands due to CO linearly bonded to exposed ruthenium atoms in very small aggregates are progressively destroyed. At the same time the bands due to a mixture of Ru_A and Ru_B species emerge, thereby indicating that the metallic phase has been oxidized. It is most noticeable that also in this experiment only Ru_A and Ru_B species are generated thus suggesting that they are very characteristic of the Ru/Al_2O_3 system. The effect of oxygen at higher T on Ru_A and Ru_B species is identical to that described in Part II and no further comment is required.

Formation of Stable Surface Aluminate Phases

A 1.57% sample previously decarbonylated *in vacuo* at 623 K and then reduced in H_2 at the same T shows the typical spectrum of adsorbed CO already discussed. After temperature treatments at 623 K the alumina surface still contains 3–4 OH/100 Å^2 which can act as potential oxidizing agents at higher T. This observation explains why after successive thermal treatments at 773 K all the manifestations of metallic ruthenium have disappeared (Fig. 7). Moreover, the Ru_A bands are now in a slightly different position, suggesting a moderate structural rearrangement favoured by the higher T. The important point to stress is that after this treatment the ions of Ru_A species become even more resistant to reduction, thereby confirming that a true surface phase has been formed.

Spectrum of Adsorbed NO

The NO molecule is, in principle, a sensitive probe (like CO) of the electronic state of the adsorbing centres, and its interaction with the dispersed ruthenium has already been studied (*5*, *23*). In particular on well-reduced samples NO initially gives rise to a nitrosylic band at 1810 cm^{-1} (*5*, *23*) and then, at higher coverages, acts as an efficient oxidizing agent of the surface. The situation is very similar in our case. The transient species absorbing at 1800–1810 cm^{-1} can be assigned to NO linearly adsorbed on Ru^0 atoms on the surface of metallic crystallites, while the band at 1840–1873 cm^{-1} can be assigned to NO on more oxidized centres. The transient nature of the band at 1800–1810 cm^{-1} can be understood if an oxidation process destroys

the initially generated $Ru^0(NO)$ complexes and forms $Ru^{x+}(NO)$ species. NO stretching bands of $Ru^{3+}(NO)$ complexes occur in the range 1873–1840 cm^{-1} (see Part II): as a consequence we conclude that upon NO exposure Ru^0 is mainly oxidized to the trivalent state. On samples oxidized at 373 K, the NO is still adsorbed in a linear form and produces a nitrosylic species absorbing at 1890 cm^{-1}. We think that this species is associated with Ru^{4+} ions, in agreement with the average tetravalent oxidation state determined by TPR experiments and with the higher stretching frequency which monitors an extremely reduced back-bonding ability.

On reduced and activated samples bands are observed at frequencies lower than 1800 cm^{-1} which were not so prominent in the published spectra of NO adsorbed on dispersed ruthenium (*5*, *23*). Having established that the NO linearly bonded to metallic crystallites is characterized by a stretching frequency in the narrow interval 1810–1800 cm^{-1}, the bands at 1700 and 1600 cm^{-1} must be assigned to bridged or to NO^- (bent) species (*16*, *24*, *25*). The latter species are frequently found in Ru complexes of ruthenium in low-valency state (*24*).

Interaction of NO with Preadsorbed CO

The first NO dose erodes preferentially the low-frequency part of the CO spectrum with formation of the nitrosylic band at 1800–1810 cm^{-1} already assigned to NO linearly bonded to zerovalent ruthenium. This fact indicates that in the first stages NO displaces CO, at least partially, from Ru^0 centres. The presence of a band at lower frequencies (1730 cm^{-1}) also suggests the presence of bridging or NO^- (bent) structures. The parallel oxidizing effect of NO is demonstrated also in this case by the initial increase of the Ru_A species. In the successive interaction stages, NO interacts also with the Ru_A species and as a consequence their concentration declines (this part of the experiment is nearly identical to that described in Part II) and no further comment is required.

CONCLUSIONS

The extent of reduction and dispersion of Ru obtained from decarbonylation of $Ru_3(CO)_{12}$ depends upon the experimental conditions adopted. In particular:

(a) samples decarbonylated *in vacuo* and then reduced in hydrogen contain a residual fraction of Ru ions mainly in trivalent state which are stabilized on the surface through the formation of a surface aluminate phase;

(b) samples decarbonylated in flowing H_2 are more reduced because the process of formation of a stable oxidized surface phase is inhibited;

(c) Ru ions act as nucleation centres for the formation of metallic particles;

(d) samples with higher Ru^{x+} content show the maximum dispersion;

(e) at 473 K and in the presence of CO, ruthenium clusters are disaggregated with formation of low-nuclearity carbonylic species;

(f) total CO desorption from samples treated in this way restores the original situation as the Ru atoms nucleate again on Ru^{x+} centres;

(g) NO is a sensitive probe of the oxidation state of supported Ru.

REFERENCES

1. Zecchina, A., Guglielminotti, E., Bossi, A., and Camia, M., *J. Catal.* **74**, 225 (1982).
2. Guglielminotti, E., Zecchina, A., Bossi, A., and Camia, M., *J. Catal.* **74**, 240 (1982).
3. Della Betta, R. A., *J. Phys. Chem.* **79**, 2519 (1975).
4. Brown, M. F., and Gonzalez, R., *J. Phys. Chem.* **80**, 1731 (1976).
5. Davydov, A. A., and Bell, A. T., *J. Catal.* **49**, 332 (1977).
6. Primet, M., Basset, J. M., Garbowski, E., and Mathieu, M. V., *J. Amer. Chem. Soc.* **97**, 3665 (1975).
7. Yermakov, Y. I., *in* "Proceedings, 7th International Congress on Catalysis, Tokyo, 1980," p. 57. Elsevier, Amsterdam, 1981.
8. Seleznev, V. N., Fomichev, Y. N., and Levinter, M. E., *Neftekhimiya* **14**, 205 (1974).
9. Defossé, C., Laniecki, M., and Burwell, R. L.,

Jr., *in* "Proceedings, 7th International Congress on Catalysis, Tokyo, 1980," p. 1331. Elsevier, Amsterdam, 1981.
10. Gault, F. G., Zahraa, O., Dartigues, J. H., Maire, G., Peyrot, M., Weisang, E., and Engelhart, P. A., *in* "Proceedings, 7th International Congress on Catalysis, Tokyo, 1980," p. 199. Elsevier, Amsterdam, 1981.
11. Tyler, R., Levenson, F., and Gray, H. B., *J. Amer. Chem. Soc.* **100,** 7889 (1978).
12. Clark, R. J. H., and Francks, M. L., *J. Chem. Soc. Dalton Trans.*, 1825 (1976).
13. Garbowski, E., Thesis, Univ. Claude Bernard, Lyon, 1976.
14. Miner, R. S., Jr., Manba, S., and Turkevich, J., *in* "Proceedings, 7th International Congress on Catalysis, Tokyo, 1980," p. 160. Elsevier, Amsterdam, 1981.
15. Chini, P., Longoni, G., and Albano, V. G., *Advan. Inorg. Chem.* **14,** 286 (1976).
16. Johnston, R. D., *Advan. Inorg. Chem. Radiochem.* **13,** 471 (1970).
17. Gomes, W., *Trans. Faraday Soc.* **59,** 1648 (1963).
18. Rohloff, E., *Z. Phys.* **132,** 643 (1952).
19. Huber, H., McIntosh, D., and Ozin, G. A., *Inorg. Chem.* **16,** 3070 (1977).
20. Ozin, G. A., *Catal. Rev. Sci. Eng.* **16,** 191 (1977).
21. Yates, D. J. C., Murrell, L. L., and Prestridge, E. B., *J. Catal.* **57,** 41 (1979).
22. Martino, G., *in* "Proceedings, 32nd International Meeting on Growth and Properties of Metal Clusters, Lyon, 1979," p. 399. Elsevier, Amsterdam, 1980.
23. Brown, M. F., and Gonzalez, R. D., *J. Catal.* **44,** 477 (1976).
24. McCleverty, J. A., *Chem. Rev.* **79,** 53 (1979).
25. Griffith, W. P., *Advan. Organomet. Chem.* **7,** 211 (1968).